QUANTUM COMPUTING IN MANY BODY PHYSICS

M.Sc. THESIS

by

Debankan Sannamoth
(Roll No.- 2103151006)

to

DEPARTMENT OF PHYSICS
INDIAN INSTITUTE OF TECHNOLOGY
INDORE - 453 552, INDIA
June, 2023

QUANTUM COMPUTING IN MANY BODY PHYSICS

A THESIS

Submitted in partial fulfilment of the requirements for the award of the degree
of
Master of Science

by
Debankan Sannamoth

DISCIPLINE OF PHYSICS
INDIAN INSTITUTE OF TECHNOLOGY, INDORE
June, 2023

INDIAN INSTITUTE OF TECHNOLOGY INDORE

CANDIDATE'S DECLARATION

I hereby certify that the work which is being presented in the thesis entitled **Quantum Computing in many body physics** in the partial fulfillment of the requirements for the award of the degree of **Master of Science** and submitted in the **Discipline of Physics, Indian Institute of Technology Indore**, is an authentic record of my own work carried out during the time period from July 2022 to June 2023 under the supervision of **Dr. Ankhi Roy, Professor, Indian Institute of Technology Indore.**

The matter presented in this thesis has not been submitted by me for the award of any other degree of this or any institute.

Debankan Sannamoth 25/5/23
Signature of the student with date
(Debankan Sannamoth)

This is to certify that the above statement made by the candidate is correct to the best of my knowledge.

Ankhi Roy 26/05/2023
Signature of the Supervisor of M.Sc. thesis (with date)
(Dr. Ankhi Roy)

DEBANKAN SANNAMOTH has successfully given his M.Sc. Oral Examination held on **Date**

Ankhi Roy
Signature of Supervisor of M.Sc. thesis
Date: 26/05/2023

Subhendu Rakshit
Convener, DPGC
Date: May 26, 2023

Signature of PSPC Member no. 1
Date: 26/05/23

Signature of PSPC Member no. 2
Date: 26/05/2023

Dipankar Das

To my family for being there during all the hardships.

Acknowledgement

Firstly, I am greatly thankful to my supervisor Dr.Ankhi Roy who has always guided me and motivated me to put an extra bit of effort into the project. She always gave the most invaluable suggestions and boosted my morale whenever I faced any kind of dispiriting hurdles and for that I am indebted to her forever.
To have Dr.Debajyoti Sarkar and Dr.Dipankar Das as my PSPC members has been the most humbling experience ever. They were always there when I needed any help or guidance.
I am extremely thankful to Dr.Mohsin Ilahi and Mr.Basit Iqbal, affiliated to Kashmiri Institute of Mathematical Sciences, India for their support and help in theoretical understanding as well as coding during the majority time of this project. Lastly, I am indebted to Dr.Rukhsan Ul Haq, IBM Quantum for being available for any discussion related to Quantum Computing whenever I needed.

Abstract

Quantum computing is based on quantum mechanics and its phenomena. It promises to provide high computational power, high speed compared to classical computers and solve unsolvable problems of classical computers. However it would take a while before we have fault-intolerant quantum computers. The most prominent application of Noisy-Intermediate Scale Quantum (NISQ) era is Variational Quantum Eigensolver (VQE) which is used to approximate ground state energy eigenvalues of various physical systems. In this thesis the main idea is to explore various aspects of Quantum Computing keeping the deuteron problem at the core, starting from its basics and slowly moving on to VQE and then studying the impact of various Quantum Noise on it. An algorithm named Subspace Search Variational Quantum Eigensolver which is also used to infer meaningful results about the excited state of deuteron. We also explore a diagonalisation technique named Schrieffer-Wolff transformation which opens door for future work.

Contents

1 Introduction **1**
- 1.1 The building blocks of Quantum Computers- Qubits 1
- 1.2 Superposition and Entanglement 2
- 1.3 Quantum circuits 2
- 1.4 Structure of the thesis 3

2 Physical Realisation of Qubits **4**
- 2.1 Ingredients to trap an ion and seperate it from surroundings 4

3 Variational Principle and Variational Quantum Eigensolver **7**
- 3.1 Mathematical Background 7
- 3.2 The Variational Quantum Eigensolver 8
  - 3.2.1 Jordan Wigner Transformation 9
- 3.3 Summarizing the VQE process 10

4 The Deuteron Problem **11**
- 4.1 Calculations and Results 11

5 Comparative study of various VQE components **14**
- 5.1 Fermionic space to spin space transformations 14
- 5.2 Generalized encodings 15
  - 5.2.1 The Jordan-Wigner encoding 16
  - 5.2.2 The Parity Encoding 16
  - 5.2.3 The Bravyi-KItaev encoding 17
- 5.3 Different Ansatzes in VQE 17
- 5.4 Entanglement pattern in the VQE circuit 18
- 5.5 Results 19

6 Subspace-search variational quantum eigensolver for excited states **22**
- 6.1 Introduction 22
- 6.2 Algorithm of Subspace-search variational quantum eigensolver 23
  - 6.2.1 Algorithm:- 23

6.3 Using SSVQM in the Deuteron Problem:- 23

7 Quantum Noise **25**
7.1 Classical noise 26
7.2 Examples of Quantum noise 27
7.2.1 Geometric picture of single qubit quantum operations 27
7.2.2 Bit flip and Phase flip 27
7.2.3 Depolarizing channel 29
7.3 Applying noise model in Deuteron simulation 31
7.3.1 Impact of a realistic noise model on binding energy . 31
7.4 Implementing our own simple noise model 34
7.4.1 All qubit depolarising noise model 34
7.4.2 All qubit bit-flip noise model 35
7.5 Remarks on the above results 35

8 A Model type approach **36**
8.1 Deuteron clustering to form Helium 36

9 Conclusion and Outlook **38**

A Schrieffer Wolff Transformation on Quantum devices **39**
A.1 Mathematical steps:- 39
A.2 Quantum Algorithm for SWT 40
A.3 Implementation of SWT and its quantum algorithm 41
A.3.1 Analytical calculation on Single Impurity Anderson model's hamiltonian 41
A.3.2 Analytical calculation on Jaynes Cummings hamiltonian in rotating wave approximation 42
A.3.3 Implementing the quantum algorithm 43
A.4 Remarks on the above results 44

List of Figures

1.1 Classical bit vs Quantum bit. 1
1.2 Creating an entangled state. 2
1.3 Few examples of Quantum gates. 2
1.4 Quantum Circuit. 3

2.1 Physical two level systems. 4
2.2 Left-a single trapped ion and Right- a superconducting qubit chip. 5
2.3 Process of trapping a Calcium ion. 6

3.1 An example of parametrized circuit. 8
3.2 Pipeline of VQE for Molecular simulation. 9
3.3 JW transformation, where σ's correspond to Pauli X,Y,Z. . . 9

4.1 Optimsed Ground state energy values of Deuteron with increasing N. 12

5.1 Ansatz-EfficientSU2, SU(2) gates-Rx, X, Qubits-3, Entanglement pattern-full. 19
5.2 Ansatz-EfficientSU2, SU(2) gates-Rz, Ry, Qubits-3, Entanglement pattern-linear. 19
5.3 Ansatz-EfficientSU2, SU(2) gates-Rz, Ry, Qubits-3, Entanglement pattern-circular. 19
5.4 Table of comparison for Two local ansatz. 20
5.5 Table of comparison for Efficient SU2 ansatz. 20
5.6 Table of comparison for Real Amplitude ansatz. 21
5.7 Comparing the evaluation counts taken by three different mappers to reach the reference value of $\langle H_4 \rangle$. The topmost plot is for Jordan Wigner mapper, the middle one is for Parity mapper while the bottom most plot is for Bravyi Kitaev mapper. 21

6.1 Value of first excited state energy of deuteron with increasing N. 24

7.1 The probabilities with which the bit may flip or remain unflipped. 26
7.2 The effect of bit flip channel for p=0.3 28
7.3 The effect of phase flip channel for p=0.3 29
7.4 The effect of bit-phase flip channel for p=0.3 29
7.5 The effect of depolarizing channel for p=0.5 30
7.6 Comparison of expectation value of hamiltonian with and without noise. 32
7.7 Comparing convergence of the expectation value of 1-qubit hamiltonian with and without noise. 32
7.8 Comparing convergence of the expectation value of 2-qubit hamiltonian with and without noise. 33
7.9 Comparing convergence of the expectation value of 3-qubit hamiltonian with and without noise. 33
7.10 Comparing convergence of the expectation value of 4-qubit hamiltonian with and without noise. 34
7.11 Comparison of expectation value of hamiltonian with and without 5% depolarising noise on all qubits. 34
7.12 Comparison of expectation value of hamiltonian with and without 5% bit-flip noise on all qubits. 35

8.1 Deuteron clustering to form Helium. 36
8.2 Ground state energy values of helium for different qubit hamiltonian 37

1 Introduction

Richard Feynman gave a speech at Caltech in 1959 named "There is plenty of room at the bottom" to motivate people to start thinking incredibly small. He believed that it is theoretically possible to simulate Quantum materials as nature by default behaves Quantum mechanically. We can simulate Quantum systems with Quantum computers. It is not a turing machine but is fundamentally different. More ideas about simulating physics using computers can be found in[1].

1.1 The building blocks of Quantum Computers-Qubits

The computational elements required for the simulation must be proportional to the space time volume of the physical system. As the system size grows in size, the computational cost grows exponentially and it becomes intractable. While a classical bit can only be in state 0 or state 1, a quantum bit can stay in a simultaneous superposition of state $|0\rangle$ and $|1\rangle$ as shown in the figure below.

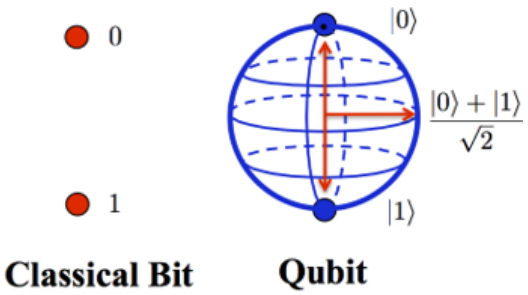

Figure 1.1: Classical bit vs Quantum bit.

1.2 Superposition and Entanglement

Superposition and Entanglement are the key features providing power to Quantum Computers to potentially solve classical intractable problems. An array of quantum bits obeys the same Quantum Mechanical laws as an wavefunction of electrons. An entangled state is one which can never be written as the tensor product of two different states. When two particles are entangled, measurement on one state reveals information about the other particle as well. In Quantum computing, we can create an entangled qubit state using Quantum gates known as Hadamard gate and CNOT gate. In the figure below we have shown an entangled qubit state also called Bell's state. It is significant to note that before any measurement is made, both the qubits have 50 percentage chance of being in state 0 or 1. However, after a measurement is made on a single qubit, it changes the probability of finding the other qubit in either of the state from 50 percentage to 100 percentage by collapsing in a particular state. Entanglement and Bell state finds application in Quantum Teleportation[2]

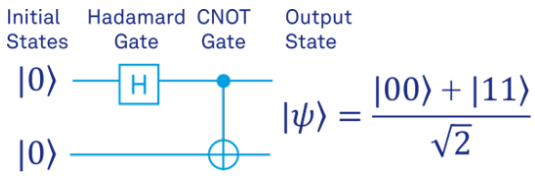

Figure 1.2: Creating an entangled state.

1.3 Quantum circuits

The two most important requisites for classical computing are classical bits and gates which does the operation on the bits. Similarly in Quantum computing, we need Quantum gates which operates on qubits. Quantum gates are unitary matrix which transform qubit from one state to another.

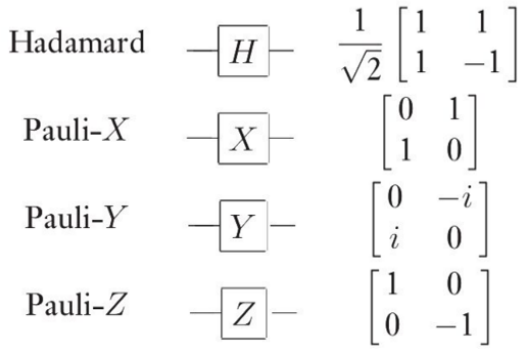

Figure 1.3: Few examples of Quantum gates.

So in a Quantum circuit the gates are applied on the input qubits to

change their state as per the requirements of computation then measurements are made to extract the information.

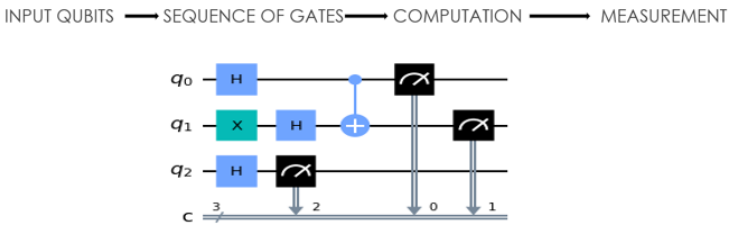

Figure 1.4: Quantum Circuit.

1.4 Structure of the thesis

This thesis is organised as follows: first we briefly talk about the physical realization of a qubit, then comes the main part of our project which is called Variational Quantum Eigensolver(VQE). We explored every aspect of VQE keeping the deuteron problem at the back of our mind. Some discussions on Quantum Noise and its impact on our simulation is also discussed in the later parts of this thesis. We even tried to extend the work by implementing Subspace Search Variational Quantum Eigensolver (SSVQE) algorithm on the deuteron problem to infer the experimental fact that deuteron has no excited state. The last chapter is dedicated to a model type approach for heavier nuclei. Finally in the appendix, a diagonalising technique named Schrieffer-Wolff transformation is discussed which opens door to our future works in this field.

2

Physical Realisation of Qubits

We can approximate any two level system as a potential qubit storing information of one state as state $|0\rangle$ and information of another state as state $|1\rangle$ say for example:-
i)The ground and excited state of an atom
ii)The horizontal and vertical polarization of light
iii)The up and down state of spin

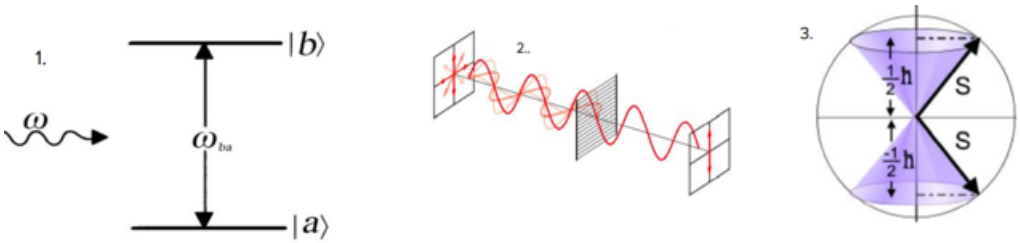

Figure 2.1: Physical two level systems.

Different hardware companies focus on different approaches for making qubits with long coherence time. The most successful ones till date are:-
i) Ion trap (used by Honeywell)
ii) Superconducting qubits (used by IBM)

Although both the qubits making involves a great detail of information and knowledge, in the next section we would briefly explain the process of trapping an ion.

2.1 Ingredients to trap an ion and seperate it from surroundings

For this technique, we mainly use Calcium atom which has 20 electrons and 20 protons. There are two valence shell electrons. If we shine a purple/blue laser, we can kick out one of the electrons and turn it into an ion.
Once it has become an ion, it is easy to manipulate using charged electrodes.

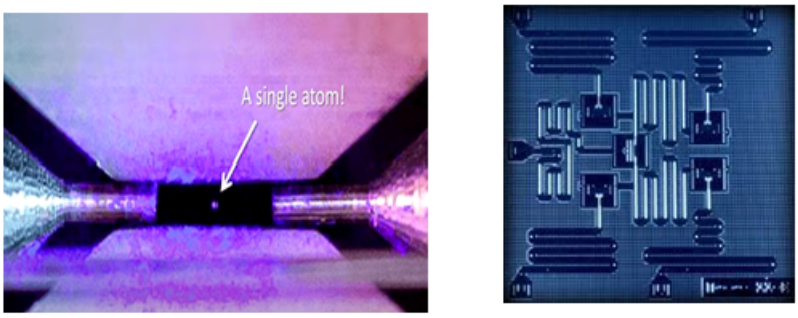

Figure 2.2: Left-a single trapped ion and Right- a superconducting qubit chip.

As we know like charges repel and unlike charges attract, so we can keep on flipping the signs of the electrodes as shown in the figure below to ensure the ion is trapped in the center. The picture of gold chip shown below has the electrodes projected on the surface and a similar configuration of charges are used to trap the ions just above it. The last picture below shows four trapped ion over a gold chip.
Now the lone outermost electron has an intrinsic property known as spin which we might think of a bar magnet. We can consider the up spin as our state $|0\rangle$ and the down spin as state $|1\rangle$ of the qubit. Now we can use microwave as an external stimulus, which being electromagnetic has constantly oscillating magnetic field. The moment of the spin starts rotating so as to align itself with the direction of the magnetic field. So depending on the time for which microwave is kept on, we might stop the spin along a direction somewhere in between up and down state. Thats a superposed state!
Note that we have to make sure the ion doesnot interact with surrounding atoms of the atmosphere so we have place the gold chip and an oven which would produce vapours of calcium atom inside an ultra-high vacuum system as shown in the figure below

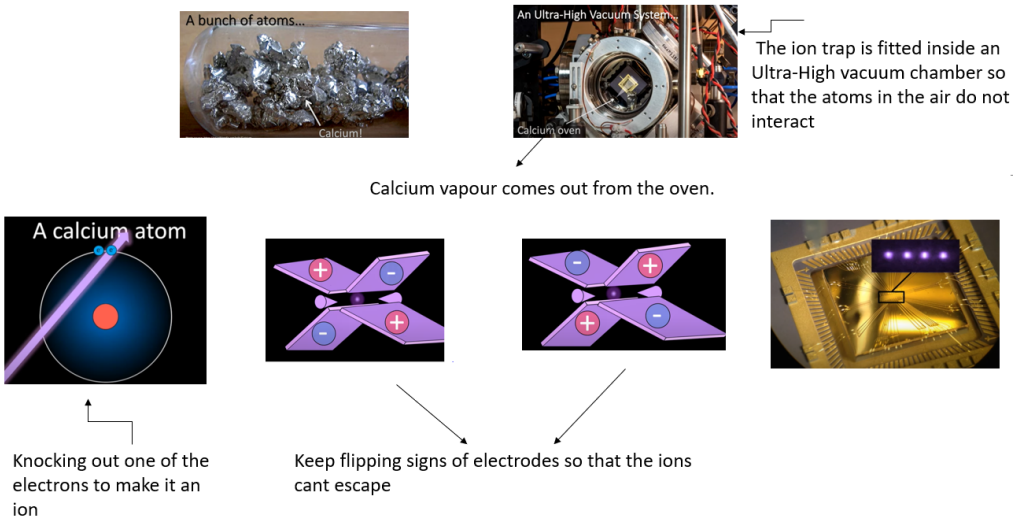

Figure 2.3: Process of trapping a Calcium ion.

3

Variational Principle and Variational Quantum Eigensolver

3.1 Mathematical Background

VQE utilizes the variational method in quantum mechanics to approximate the eigenvectors and eigenvalues of a given matrix, such as matrix A. The eigenvector, denoted as $|\psi_i\rangle$, remains unchanged up to a scalar multiple when transformed by matrix A, where the corresponding eigenvalue is represented by λ_i.

$$A|\psi_i\rangle = \lambda_i|\psi_i\rangle \tag{3.1}$$

Furthermore a matrix H is said to be hermitian if its equal to its own conjugate transpose

$$H = H^\dagger \tag{3.2}$$

The spectral theorem states that eigenvalues associated with a Hermitian matrix, such as matrix H, are always real numbers. Therefore, any eigenvalue, denoted as λ_i, possesses the property that it is equal to its complex conjugate, represented as $\lambda_i = \lambda_i^\dagger$. This property arises from the requirement that any physically measurable quantity must be real. Hence, hermitian matrices provide a suitable mathematical framework for describing the hamiltonians of quantum systems. Moreover H may be expressed as

$$H = \sum_{i=1}^{N} \lambda_i|\psi_i\rangle\langle\psi_i| \tag{3.3}$$

where λ_i is the eigenvalue corresponding to each ψ_i. The expectation value of H can be written as

$$\langle H\rangle_\psi = \langle\psi|H|\psi\rangle \tag{3.4}$$

Substituting H as the weighted sum of its eigenvectors it can be shown that

$$\langle H\rangle_\psi = \langle\psi| \left(\sum_{i=1}^{N} \lambda_i|\psi_i\rangle\langle\psi_i| \right) |\psi\rangle$$

(3.5)

$$\langle H\rangle_\psi = \sum_{i=1}^{N} \lambda_i \langle\psi|\psi_i\rangle\langle\psi_i|\psi\rangle \tag{3.6}$$

$$\langle H\rangle_\psi = \sum_{i=1}^{N} \lambda_i |\langle\psi_i|\psi\rangle|^2 \tag{3.7}$$

The above equation states that the expectation value of an observable on any state can be expressed as a linear combination using the eigenvalues associated with H as weights. Moreover each of the weights in the linear combination is greater than or equal to 0 as $|\langle\psi_i|\psi\rangle|^2 \geq 0$ so it is clear that

$$\lambda_{min} \leq \langle H\rangle_\psi = \langle\psi|H|\psi\rangle = |\langle\psi_i|\psi\rangle|^2 \tag{3.8}$$

where we have considered $|\psi\rangle$ to be normalised. This is the Variational Principle.

When the hamiltonian of the system is described by a hermitian matrix H then the lowesst eigen value E_{gs} is the ground state energy value. We can select any wavefunction $|\psi_i\rangle$ as the initial guess trial wavefunction (also called ansatz), calculate the expectation value of the hamiltonian and then iteratively update the wavefunction to reach the minimum posssible eigenvalue.

3.2 The Variational Quantum Eigensolver

We repeat the same exact procedure with an initial guess of ansatz using a parametrized circuit in quantum computer. Such a circuit is also called a variational form and its action is represented as an unitary transformation $U(\theta)$ acting on the on the vacuum state of qubits $|0\rangle$ or Hartree fock state to generate $|\psi(\theta)\rangle$.

$$U(\theta)|\psi\rangle = |\psi(\theta)\rangle \tag{3.9}$$

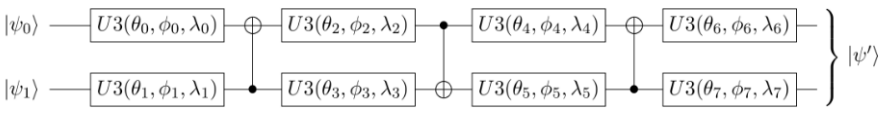

Figure 3.1: An example of parametrized circuit.

The step wise requisites which are required to solve any problem in VQE is as follows:-

i)Operator (Hamiltonian in our case) in the second quantized form.

ii)Map the second quantized form into Pauli operators.

iii)Parameterised circuit to do the unitary operation on the initial state.

iv)A classical optimizer to optimise the value of the parameter which minimises the expectation value of $\langle\psi(\theta)|H|\psi(\theta)\rangle$.

This clearly implies VQE is a hybrid algorithm where we create the parametrized ansatz using quantum computer and calculate the expectation value of H and then the parameter θ is optimized by classical optimizer to reach a $|\psi(\theta)\rangle$ which corresponds to the lowest energy eigenvalue.

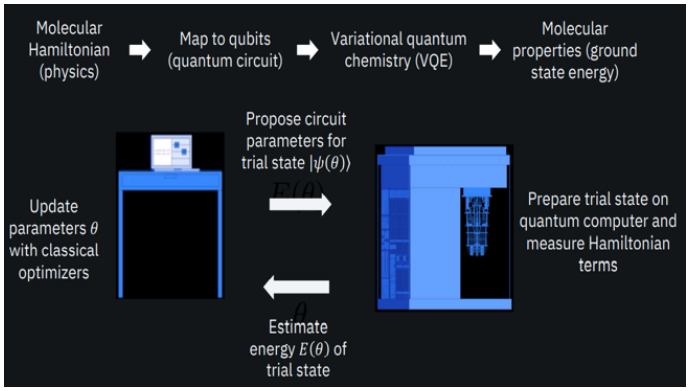

Figure 3.2: Pipeline of VQE for Molecular simulation.

3.2.1 Jordan Wigner Transformation

To enable the implementation of second-quantized hamiltonians on a quantum computer, a mapping is required to express the creation ($a^\dagger$) and annihilation (a) operators in terms of unitary matrices. In this case, the Pauli matrices (X, Y, Z, I) serve as the appropriate unitary matrices for this purpose. The Jordan Wigner mapping gives such a map[3].The main advantage of Jordan Wigner mapping over other types of mapping such as Bravyi–Kitaev representation is its simplicity. It is easy to verify the transformation rule given in the figure below.

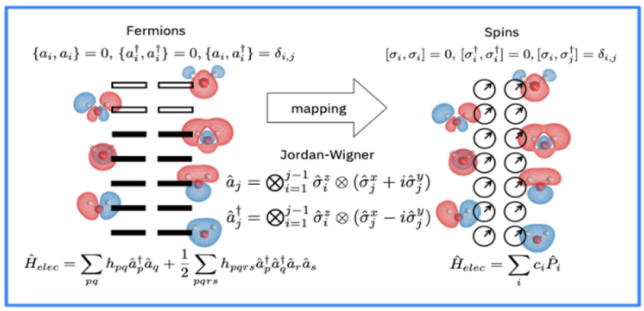

Figure 3.3: JW transformation, where σ's correspond to Pauli X,Y,Z.

3.3 Summarizing the VQE process

From the above discussions it is clear that VQE is one of the most prominent applications of NISQ era. The starting point is the hamiltonian(H) which is given as an input. It should however be noted that the hamiltonian should be converted in the form of Pauli operators which is the form understood by quantum computers. The second most crucial step as we have seen above is the preparation of the parametrised wavefunctions through the circuit where an unitary operation $U(\theta)$ is done over the state of input qubits $|\psi\rangle$ to convert it to $|\psi(\theta)\rangle$. Once we have the H in the desired form along with $|\psi(\theta)\rangle$, we take the expectation value $\langle H\rangle_\theta = \langle\psi(\theta)|H|\psi(\theta)\rangle$. Upto this is done by the quantum computer. Next a classical optimizer optimises the value of θ to give us a $|\psi(\theta)\rangle$ for which the expectation value of the of H is the lowest. Here the variational principle is used as we know that whatever may be the value of θ we would always have an expectation value whose lower bound is the ground state energy of the physical system. So in conclusion we understand that it is purely a hybrid algorithm where both quantum and classical computing is involved.

4

The Deuteron Problem

In this section we talk about the Quantum Computation of deuteron, a bound state consisting of a neutron and a proton. It is the simplest example to study nucleon-nucleon interaction. First we used the hamiltonian in second quantised form from the reference paper[4]. Substituting the experimental values and doing JW transformation, we converted the hamiltonian in the form of Pauli operator. Then we designed variational ansatz and used an optimizer in the IBM platform. The entire thing was created and coded on Qiskit. We used VQE principle to get the ground state energy eigenvalues by increasing the number of qubits which has a one isto one correspondence with the dimension of harmonic oscillator basis. Below are shown the steps and the results of simulation.

4.1 Calculations and Results

$$H_N = \sum_{n,m=0}^{N-1} \langle m|(T+V)|n\rangle a_m^\dagger a_n a \tag{4.1}$$

$$\langle m|T|n\rangle = \frac{\hbar\omega}{2}\left[(2n+3/2)\delta_n^m - \sqrt{n(n+1/2)}\delta_n^{m+1} - \sqrt{(n+1)(n+3/2)}\delta_n^{m-1}\right]$$

$$\langle m|V|n\rangle = V_0\delta_n^0\delta_n^m \tag{4.2}$$

where V_0=-5.68658111MeV (experimentally)
Using JW transformation given below

$$a_n^\dagger = \frac{1}{2}\left[\prod_{k=0}^{n-1} Z_k\right](X_n - iY_n) \tag{4.3}$$

$$a_n = \frac{1}{2}\left[\prod_{k=0}^{n-1} Z_k\right](X_n + iY_n) \tag{4.4}$$

Doing the necessary steps by increasing the value of n,m we get the below expressions for hamiltonian.

For **N=1:-**

$$H_1 = \frac{3\hbar\omega}{8}(I - Z_0) + \frac{V_0}{2}(I - Z_0)$$

For **N=2:-**

$$H_2 = \frac{3\hbar\omega}{8}(I - Z_0) + \frac{V_0}{2}(I - Z_0) + \frac{\hbar\omega}{4}\sqrt{\frac{3}{2}}(X_0X_1 + Y_0Y_1) + \frac{7\hbar\omega}{8}(I - Z_1)$$

For**N=3:-**

$$H_3 = \frac{3\hbar\omega}{8}(I - Z_0) + \frac{V_0}{2}(I - Z_0) + \frac{\hbar\omega}{4}\sqrt{\frac{3}{2}}(X_0X_1 + Y_0Y_1) + \frac{7\hbar\omega}{8}(I - Z_1) - \frac{\sqrt{5}\hbar\omega}{8}(X_1X_2 + Y_1Y_2) + \frac{11\hbar\omega}{8}(I - Z_2)$$

For **N=4:-**

$$H_4 = \frac{3\hbar\omega}{8}(I - Z_0) + \frac{V_0}{2}(I - Z_0) + \frac{\hbar\omega}{4}\sqrt{\frac{3}{2}}(X_0X_1 + Y_0Y_1) + \frac{7\hbar\omega}{8}(I - Z_1) - \frac{\sqrt{5}\hbar\omega}{8}(X_1X_2 + Y_1Y_2) + \frac{11\hbar\omega}{8}(I - Z_2) - \frac{\hbar\omega}{4}\sqrt{\frac{21}{2}}(X_2X_3 + Y_2Y_3) + \frac{15\hbar\omega}{8}(I - Z_3)$$

Similar calculations were done upto N=5 with $\hbar\omega = 7MeV$ using the concept of cutoff [5][6] and the expression of hamiltonian keeps getting longer and corresponding depth of circuit also increases with the number of qubits.
The results of the simulation are given in the table below

Value of N	Value of Ground state energy(MeV)
1	-0.43
2	-1.74
3	-2.04
4	-2.14
5	-2.18

Figure 4.1: Optimsed Ground state energy values of Deuteron with increasing N.

It is evident that with increasing N, the value approaches the experimental value of deuteron ground state energy which is $-2.22MeV$. The accuracy of the results are indeed very satisfactory.

5

Comparative study of various VQE components

After simulating the deuteron problem using VQE successfully in the previous chapter, we started exploring various ansatzes, encoding and entanglement type between qubits in the circuit which are available in Qiskit. We explored different combinations of ansatzes with various entangling patterns to compare which one converges to the reference value faster. On top of that we used three different encoding or mapping techniques to map the hamiltonian from creation and annihilation form to pauli operators to compare the results. Before we list the result, lets understand the theory behind different methods a bit.

5.1 Fermionic space to spin space transformations

A parameterized ansatz wavefunction is used to evaluate the expectation value of the Hamiltonian operator at the heart of the VQE algorithm. Second quantization is favoured over first quantization in the current era of Noisy Intermediate-Scale Quantum (NISQ) devices, which have limited qubit resources. Following the guidelines of anti-commutation algebra, the fermionic creation and annihilation operators are used in second quantization. These operators allow for a concise representation of many-particle quantum states and facilitate the analysis of complex following the guidelines of anti-commutation algebra, the fermionic creation and annihilation operators are used in second quantization.ermionic systems within the VQE framework.

In contrast to classical bits, qubits are spin-1/2 entities and serve as the fundamental units of measurement on Quantum Processing Units (QPUs). The Pauli X, Y, and Z operators, which act on qubits, follow a distinct algebra defined by their Lie bracket. Consequently, in the VQE algorithm, it becomes necessary to convert the hamiltonian from its second quantization representation into a linear combination of Pauli strings. These

Pauli strings consist of tensor products of Pauli operators acting on multiple qubits. This transformation enables the efficient utilization of qubits for the measurement and manipulation of quantum states within the VQE loop.

It is important to highlight that operators in second quantization must satisfy the requirements of wavefunction antisymmetry and anti-commutation rules. Unlike Pauli operators, which do not inherently adhere to these relationships, special considerations must be taken when mapping fermionic operators in the context of second quantization. The transformation involves mapping the operator space, acting on a Fock space with "n" orbitals, to a Hilbert space with a dimension of "2n". Interestingly, well before the advent of quantum computers, Jordan and Wigner demonstrated the existence of one to one map between fermionic space and qubit space, preserving the desired algebraic structure. This insight has paved the way for establishing the connection between fermionic systems and qubit-based quantum computing approaches.

The factors that help us in deciding a specific encoding are as follows:-

1)**Number of qubits**:The number of spin-orbitals or sites taken into account in a quantum simulation often determines the number of qubits required. However, a number of methods have been devised to compress and combine the data held within the wavefunction onto a smaller number of qubits. These techniques leverage the symmetries inherent in the Hamiltonian under study. By exploiting these symmetries, it becomes possible to reduce the number of qubits needed for an accurate representation of the system, enabling more efficient quantum simulations and computations.

2)**Pauli weight**: The biggest count of non-identity operators in any mapped Pauli string, which is the maximum number of qubits that are impacted by any Pauli string.

3)**Number of Pauli-strings**: The count of distinct Pauli strings obtained through the mapping process. The quantity of Pauli strings significantly influences the computational overhead of implementing VQE. Therefore, all else being equal, it is preferable to minimize the number of Pauli strings to be measured, aiming for computational efficiency.

5.2 Generalized encodings

Our attention is directed towards encodings that encompass the entire Fock space, which corresponds to the domain of the hamiltonian. The number of qubits, denoted as N, required for such encodings is theoretically equivalent to the number of spin orbitals, represented as n, present in the hamiltonian (excluding any potential reductions due to symmetries).These encodings are agnostic to specific hamiltonian structures and provide a general ap-

proach for representation and manipulation of quantum systems.

5.2.1 The Jordan-Wigner encoding

The Jordan-Wigner encoding technique transforms the electronic wavefunction into an array of qubits by linking the occupation number of spin orbitals to the states of the qubits. To be more precise, "N" qubits are used to represent the number of spin-orbitals that are occupied by "n." The state $|0\rangle_j$ indicates the j-th orbital is unoccupied, while $|1\rangle_j$ signifies the j-th orbital being occupied. Here, the index "j" combines the spatial and spin orbital indices, providing a unified representation within the encoding scheme.

In the scenario of a single orbital, the actions of fermionic operators on the j-th qubit can be expressed as spin operators as :

$$a_j^\dagger = \begin{bmatrix} 0 & 0 \\ 0 & 1 \end{bmatrix} = \frac{X_j - iY_j}{2}$$

$$a_j = \begin{bmatrix} 0 & 1 \\ 0 & 0 \end{bmatrix} = \frac{X_j + iY_j}{2}$$

where X_j and Y_j are Pauli gates acting on the j-th qubit. The fermionic anticommutation relation is not by default enforced by the Pauli operators. Including a series of Z operators that operate on all the other qubits before the j-th location is one way to tackle this problem. This additional set of Z operators ensures that states with eigenvalues of +1 correspond to those that have an even number of inhabited orbitals up to the j-th position and those with eigenvalues of -1 to those that have an odd number of inhabited orbitals up to the j-th position. This restoration of the fermionic sign prescription accounts for the necessary anticommutation properties within the encoded fermionic system. So ultimately the Jordan-Wigner transformation is as follows

$$a_j^\dagger = \frac{X_j - iY_j}{2} \otimes Z_0 \otimes ... \otimes Z_{j-1} \tag{5.1}$$

$$a_j = \frac{X_j + iY_j}{2} \otimes Z_0 \otimes ... \otimes Z_{j-1} \tag{5.2}$$

As Z_j anticommutes with X_j and Y_j, one can easily check that this modification ensures that the fermionic anticommutation relations among creationa nd annihilation operator is restored that is now we have $a_i a_j^\dagger = -a_j^\dagger a_i$ for $i \neq j$

5.2.2 The Parity Encoding

We can achieve a concept known as parity encoding by using the j-th qubit to encode data related to the orbital's parity till the j-th position rather than immediately signalling the occupancy of the j-th orbital. The state $|0\rangle_j$ denotes an even number of inhabited orbitals up to and including the

j-th position in this encoding method, whereas $|1\rangle_j$ denotes an odd number of filled orbitals.

Given this definition, if we are provided with the fermionic state $|v_0 v_1 .... v_n\rangle$, we can translate it into the qubit state $|p_0 p_1 .... p_n\rangle$ within the parity encoding framework by applying the following mapping:

$$p_i = \sum_j v_j \tag{5.3}$$

When the parity of the j-th qubit changes, meaning a transition occurs from $|0\rangle_{j-1}$ to $|1\rangle_j$ or from $|1\rangle_{j-1}$ to $|0\rangle_j$, it indicates that the j-th orbital is inhabited. In contrast, if the parity remains unchanged, then the j-th orbital is unoccupied.

The encoding of information regarding the parity of qubits up to the j-th position is performed in the (j-1)-th qubit.When the (j-1)th qubit is in the state $|1\rangle_{j-1}$, the fermionic operators a_j and $a_j^\dagger$ introduce a minus sign, and when it is in the state $|0\rangle_{j-1}$, a plus sign. This enables us to establish the mapping for isolated fermionic operators as follows:

$$a_j^\dagger = \frac{Z_{j-1} \otimes X_j - iY_j}{2}$$

$$a_j = \frac{Z_{j-1} \otimes X_j + iY_j}{2}$$

However, the parity recorded in the succeeding qubits that follow the j-th location must also be adjusted appropriately when an electron is added to or removed from the j-th orbital. This update involves flipping those qubits to reflect the revised parity. To achieve this, a string of X operators can be employed. Thus, the transformation of parity is expressed as follows:

$$a_j^\dagger = \frac{Z_{j-1} \otimes X_j - iY_j}{2} \otimes X_{j+1} \otimes .... \otimes X_{n-1}$$

$$a_j = \frac{Z_{j-1} \otimes X_j + iY_j}{2} \otimes X_{j+1} \otimes .... \otimes X_{n-1}$$

5.2.3 The Bravyi-KItaev encoding

Let's briefly delve into the concept behind this encoding, which involves a complex mapping process.

The primary objective of this encoding is to reduce the Pauli weight associated with the qubit operators. This is achieved by storing a combination of parity and occupation numbers within the qubits.

5.3 Different Ansatzes in VQE

The most important part of VQE is the unitary circuit which forms our wavefunction over which the expectation value of the hamiltonian terms

are measured. There are some ansatzes available in Qiskit. We explored few of them to see the rate of covergence of the expectation value to the reference value. Below are three of them which was explored:-

1) **Two Local**:-The two-local circuit is a parameterized circuit that comprises alternating layers of rotation and entanglement operations. In the rotation layers, single-qubit gates are applied to each qubit in the circuit. The entanglement layer utilizes two-qubit gates to entangle the qubits according to a specified entanglement strategy. The choice of rotation and entanglement gates can be specified using different formats such as strings (e.g., 'ry' or 'cx'), gate types (e.g., RYGate or CXGate), or even as complete quantum circuits (e.g., a circuit with one qubit or a circuit with two qubits).

2)**Efficient SU2**:-The EfficientSU2 circuit is composed of layers that involve both single-qubit operations from the special unitary group SU(2) and entanglement operations. This circuit pattern serves as a heuristic approach for preparing trial wave functions in variational quantum algorithms or constructing classification circuits for machine learning tasks.

In SU(2), which represents the special unitary group of degree 2, the elements are 2×2 unitary matrices with a determinant of 1. These elements include familiar gates like the Pauli rotation gates, which play a crucial role in the EfficientSU2 circuit.

3)**Real Amplitudes ansatz**:The RealAmplitudes circuit is a commonly employed heuristic trial wave function used as an Ansatz in various applications, such as chemistry simulations and machine learning classification circuits. This circuit is structured with alternating layers of Y-rotations and CX-entanglements.

The entanglement pattern within the RealAmplitudes circuit can either be user-defined or selected from a predetermined set. The name "RealAmplitudes" stems from the characteristic that the resulting quantum states prepared by this circuit exclusively possess real amplitudes, with a complex part that is always zero.

5.4 Entanglement pattern in the VQE circuit

In the context of the variational circuit, one can select from a range of available options, such as the Efficient SU2 circuit provided by Qiskit. By utilizing this method, it becomes possible to construct a variational circuit consisting of SU(2) gates, including well-known gates like Pauli X, Y, and Z, as well as arbitrary rotation gates (rx, ry, rz). Between the layers of the circuit, cx gates are applied to introduce entanglement among the qubits, thereby enhancing the expressive power of the variational model.

We are allowed to specify the entanglement structure. Assuming that we have N qubits in the system, the available options are:

1) **Full**- each qubit q_n is entangled using a C-X gate q_m for $m = n + 1.....N$.

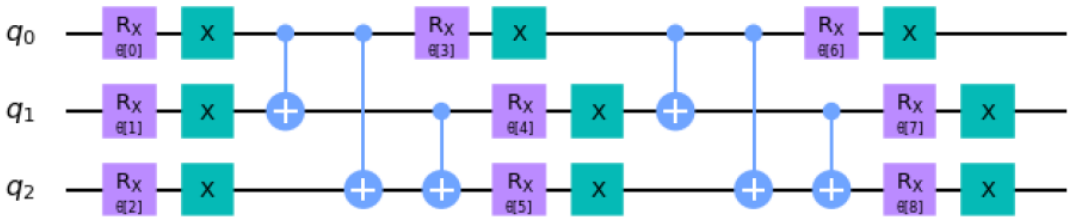

Figure 5.1: Ansatz-EfficientSU2, SU(2) gates-Rx, X, Qubits-3, Entanglement pattern-full.

2) **Linear**- each qubit q_n is entangled using a C-X gate q_m for $m = n+1$.

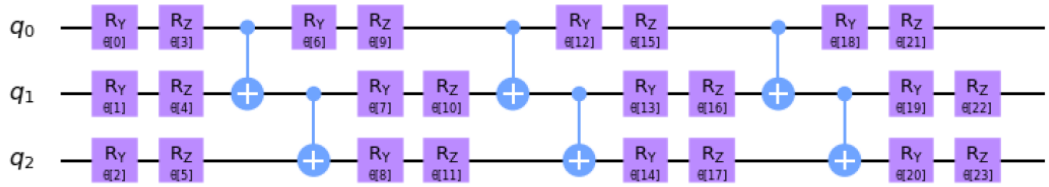

Figure 5.2: Ansatz-EfficientSU2, SU(2) gates-Rz, Ry, Qubits-3, Entanglement pattern-linear.

3) **Circular**- It is similar to 'linear' but also entangling the first and last qubit together using CX-gate.

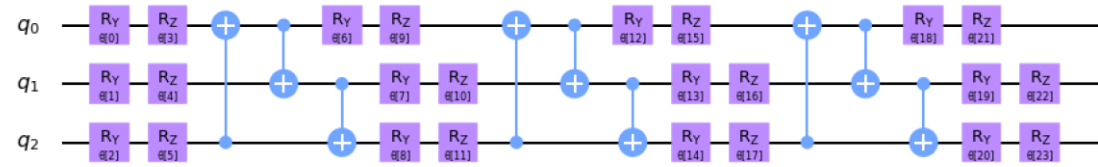

Figure 5.3: Ansatz-EfficientSU2, SU(2) gates-Rz, Ry, Qubits-3, Entanglement pattern-circular.

5.5 Results

In the tables below we compare the results of convergence to reference binding energy for the above three types of ansatzes with varying encoding and varying entanglement pattern. It is evident from the tables below that Jordan Wigner mapper gives best result when the entanglement pattern of CX gates are circular. Finally, I show below a plot comparing the number of counts taken by three different mappers to converge to the reference value

of energy for 4-qubit hamiltonian. It clearly shows that Jordan Wigner mapper produces the best result in least number of counts. This validates our decision of choosing Jordan Wigner for the initial parts of this thesis as a correct decision.

Serial No.	Ansatz	Mapper	Rotation gates	Entanglement pattern	No. of evaluations required to reach reference B.E of 4 qubit hamiltonian
1.	Two local	Bravyi Kitaev	Rz , Ry	Full	2220
				Circular	4166
				Linear	4065
		Jordan Wigner	Rz , Ry	Full	4149
				Circular	1931
				Linear	4162
		Parity	Rz , Ry	Full	3096
				Circular	3866
				Linear	4168

Figure 5.4: Table of comparison for Two local ansatz.

Serial No.	Ansatz	Mapper	Rotation gates	Entanglement pattern	No. of evaluations required to reach reference B.E of 4 qubit hamiltonian
2.	Efficient SU2	Bravyi Kitaev	Rz , Ry	Full	3990
				Circular	4152
				Linear	3661
		Jordan Wigner	Rz , Ry	Full	4139
				Circular	1686
				Linear	4157
		Parity	Rz , Ry	Full	3288
				Circular	4075
				Linear	4165

Figure 5.5: Table of comparison for Efficient SU2 ansatz.

Serial No.	Ansatz	Mapper	Rotation gates	Entanglement pattern	No. of evaluations required to reach reference B.E of 4 qubit hamiltonian
3.	Real Amplitude	Bravyi Kitaev	Ry	Full	1007
				Circular	1083
				Linear	1741
		Jordan Wigner	Ry	Full	1247
				Circular	553
				Linear	911
		Parity	Ry	Full	1745
				Circular	894
				Linear	1980

Figure 5.6: Table of comparison for Real Amplitude ansatz.

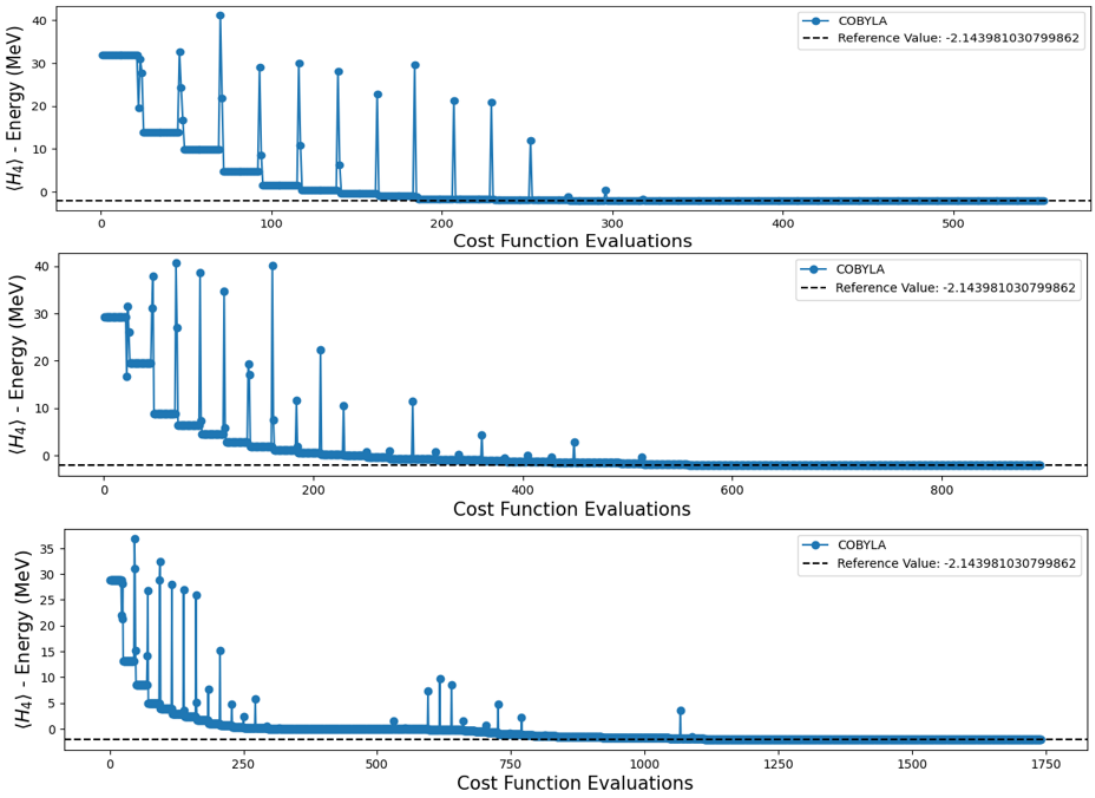

Figure 5.7: Comparing the evaluation counts taken by three different mappers to reach the reference value of $\langle H_4 \rangle$. The topmost plot is for Jordan Wigner mapper, the middle one is for Parity mapper while the bottom most plot is for Bravyi Kitaev mapper.

6

Subspace-search variational quantum eigensolver for excited states

6.1 Introduction

VQE, as a variational algorithm, holds significant promise for near-term quantum computers as it enables the approximate determination of ground states for a given Hamiltonian. This application extends beyond ground states to encompass excited states of molecules, which play crucial roles in various chemical and physical phenomena. Understanding the transitions between ground and excited states, for example, sheds light on the fundamental processes underlying phenomena such as luminescence. Therefore, VQE offers a valuable tool for exploring and characterizing a broader range of quantum states beyond just ground states.

Given the increasing computational cost and relatively poor results obtained by classical computation when it comes to analyzing excited states, the motivation to leverage quantum computers for this task arises. Quantum computers offer the potential to overcome these challenges and provide more accurate solutions.

In the context of NISQ devices, the conservation of unitary transformation is harnessed to identify excited states. The Subspace Search Variational Quantum Eigensolver (SSVQE) algorithm is employed, which takes two or more orthogonal states as inputs and utilizes a parametrized quantum circuit. The objective is to minimize the expectation value of the energy within the space spanned by these states. By ensuring the orthogonality of the output states, the SSVQE algorithm facilitates the discovery of the k-th excited state through optimization of the circuit parameters, which only needs to be performed twice. This approach greatly enhances the efficiency and accuracy of finding excited states using NISQ devices.[7].

6.2 Algorithm of Subspace-search variational quantum eigensolver

The key idea is to establish orthogonality at the input of the quantum circuit instead of the output. The algorithm for identifying the k-th excited state on an n-qubit quantum computer involves a series of steps. It is essential to emphasize that, within this context, the ground state is regarded as the 0-th excited state.

6.2.1 Algorithm:-

1.Construct an ansatz circuit $U(\theta)$ and choose input states $|\phi_j\rangle$ where j=0....k which are orthogonal ($\langle\phi_i|\phi_j\rangle = \delta_{ij}$).
2.Minimize $L_1(\theta) = \sum_{j=0}^{k}\langle\phi_j|U^\dagger(\theta)HU(\theta)|\phi_j\rangle$.We denote the optimal value of θ as θ^*.
3.Construct another parametrized quantum circuit $V(\phi)$ that only acts on the space spanned by $|\phi_j\rangle_{j=0}^{k}$.
4.Choose an arbitrary index $s\epsilon 0, ...k$ and maximize
$L_2(\phi) = \langle\phi_s|V^\dagger(\phi)U^\dagger(\theta^*)HU(\theta^*)V(\phi)|\phi_s\rangle$.

In practice the orthogonal states $|\phi_j\rangle_{j=0}^{k}$ are chosen from a set of easily preparable othogonal states such as the computational basis.

In short what we are doing is that for n qubit quantum computer we would have 2^n eigenstates for Hamiltonian H. As hermitian operators have orthogonal eigenstates so supplying different orthogonal states as input and then taking the expectation values, we are getting distinct energy eigenvalues of the Hamiltonian. In step-2, we are using VQE for each input state to get the optimized values which gives the set of distinct energy eigenvalues like ground state, first excited state , second excited state and so on till kth excited state. In step-3 we search for the maximum value out of the set of energy eigenvalues which is our k-th excited state. Ultimately by using a two step optimization process we can extract our kth excited state.

6.3 Using SSVQM in the Deuteron Problem:-

Next we tried to implement this SSVQM algorithm on the deuteron problem to see the result of the first excited state. We followed the steps discussed above starting from the hamiltonian in the second quantized form.The results upto 5 qubits hamiltonian are given below

We notice that the results of the ground state matches well with the reference values and with the values of the VQE results in Chapter 4. On the other hand, the observation that there are no excited states of deuteron aligns with experimental findings. Deuteron is a weakly bound system, and the only "excited state" it possesses is an unbound configuration comprising a free proton and a free neutron. The deuteron ground state represents the

Value of N in Hamiltonian	Ground state energy in MeV (using simulator)	First excited state energy in MeV (using simulator)
1	-0.43	5.26e-06
2	-1.74	7.57e-05
3	-2.04	9.42e-03
4	-2.14	4.21e-02
5	-2.18	3.54e-01

Figure 6.1: Value of first excited state energy of deuteron with increasing N.

sole stable bound system composed of two nucleons. Therefore, the absence of excited states in the deuteron is consistent with experimental evidence.

7 Quantum Noise

Thus far, our focus has primarily been on the dynamics of closed quantum systems, which do not experience any undesired interactions with the external environment. While we can derive fascinating insights about the potential information processing capabilities of these ideal systems, it is important to acknowledge that real-world systems are never perfectly closed, with the possible exception of the entire universe.

Quantum information processing systems in real-world settings unavoidably experience undesired interactions with the external environment, leading to the emergence of noise in the system. To construct practical and effective quantum information processing systems, it becomes essential to comprehend and manage these noise processes. Understanding and controlling noise are vital components in the development of reliable and efficient quantum information processing systems.[8][9].

How can we tell an open system from a closed one? Consider a nearly ideal closed system, such as a swinging pendulum like those used in mechanical clocks. The pendulum exhibits minimal interaction with its surroundings, primarily through friction. However, to fully capture the pendulum's dynamics and elucidate the reasons behind its eventual cessation, it is vital to take into account the dampening effects brought on by air friction and flaws in its suspension system.

Likewise, quantum systems, including quantum computers, can never achieve perfect isolation. For a desired series of operations, quantum computers rely on exact programming from an external source. For instance, if an electron's locations are used to represent the state of a qubit, interactions with other charged particles are bound to occur, leading to unavoidable noise that affects the qubit's state.

An open system is essentially one that interacts with another system, typically referred to as the environment. In the case of open quantum systems, we often wish to neglect or average over the dynamics of the environment while focusing on the system of interest. It is important to

acknowledge these interactions with the environment as they can introduce noise and undesired effects in quantum systems.

7.1 Classical noise

To enhance our comprehension of quantum noise, it can be beneficial to develop an intuitive understanding of noise in classical systems. Let's consider the scenario of storing a bit on a hard drive connected to a conventional computer. Initially, the bit is in a well-defined state of either 0 or 1. However, as time progresses, there is an increasing likelihood of stray magnetic fields interfering with the bit, potentially causing it to become scrambled or flip its state. This situation can be represented by assigning a probability, denoted as p, for the bit to flip, and a complementary probability of $1 - p$ for the bit to remain unchanged. The accompanying figure illustrates this concept:

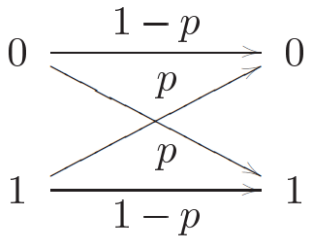

Figure 7.1: The probabilities with which the bit may flip or remain unflipped.

The conditional probabilities of the bit flipping to a particular state when it was initially in a particular state are called transitional probabilities. Writing these equations explicitly for the bit on the hard drive we get

$$\begin{bmatrix} q_0 \\ q_1 \end{bmatrix} = \begin{bmatrix} 1-p & p \\ p & 1-p \end{bmatrix} \begin{bmatrix} p_0 \\ p_1 \end{bmatrix} \tag{7.1}$$

In conclusion, the framework of stochastic procedures can be used to characterise noise in classical systems. When examining processes with multiple stages, it is often appropriate to assume Markov processes, where the noise at each step operates independently of the environment. This implies that the noise introduced into the system by various sources or components remains unaffected by the behavior of other sources or components. In the context of faulty gates, the performance of each gate is entirely independent of whether other gates are functioning correctly or not.

The matrix in equation 6.1, when multiplied with vector $\vec{p}$, is referred to as the evolution matrix (E). The evolution matrix exhibits two crucial properties. Firstly, all entries of E must be non-negative, satisfying the positivity requirement. This condition ensures that negative probabilities cannot arise from the product $E\vec{p}$. Secondly, all columns of E must sum to

one, fulfilling the completeness requirement. If this condition were violated, for instance, if the first column did not sum to one, the product $\vec{E}\vec{p}$ would not represent a valid probability distribution.

To summarize, the fundamental attributes of classical noise can be summarized as follows: a linear correlation between input and output probabilities, regulated by a transition matrix with non-negative entries (positivity) and columns that sum up to one (completeness). Assuming that the noise is influenced by separate surroundings, Markov processes can be used to characterise classical noise processes with many stages. These crucial characteristics have significant counterparts in the domain of quantum noise. However, quantum noise also introduces unique and intriguing properties of its own.

7.2 Examples of Quantum noise

Quantum systems are susceptible to various types of errors beyond simple bit flips. One such type is phase errors, which arise due to continuous evolution of the quantum state. While the overall phase is unimportant, relative phases play a crucial role. In addition to bit and phase flip error channels, we will explore the concept of depolarizing channels and delve into their geometrical interpretation. By understanding these error channels, we can gain insights into the mechanisms that introduce errors in quantum states and devise strategies to mitigate their impact.

7.2.1 Geometric picture of single qubit quantum operations

There exists a visually appealing geometric approach to visualize single qubit's quantum operations. This method provides an intuitive understanding of how quantum operations affect the qubit's state by considering their impact on the Bloch sphere. The state of a single qubit can be elegantly represented as a point on the Bloch sphere, offering a comprehensive depiction of its quantum properties.

$$\rho = \frac{I + \vec{r}.\vec{\sigma}}{2}$$

where r is the three component real vector and σs are the Pauli matrices. It is revealed that any trace-preserving quantum operation (ϵ) can be expressed as an equivalent map of the following form.

$$\vec{r} \xrightarrow{\epsilon} \vec{r'} = M\vec{r} + \vec{c}$$

where M is a 3×3 real matrix which generally takes into account the deformation and rotation of the Bloch sphere and $\vec{c}$ is a constant vector.

7.2.2 Bit flip and Phase flip

The geometric picture helps in visualizing the impact of noise on quantum state and becomes very important in quantum information theory. The bit

flip channel flips the state of a qubit from $|0\rangle$ to $|1\rangle$ (and vice versa) with probability $1-p$. It has operation elements

$$E_0 = \sqrt{p}I = \sqrt{p}\begin{bmatrix}1 & 0\\ 0 & 1\end{bmatrix}, E_1 = \sqrt{1-p}X = \sqrt{1-p}\begin{bmatrix}0 & 1\\ 1 & 0\end{bmatrix}$$

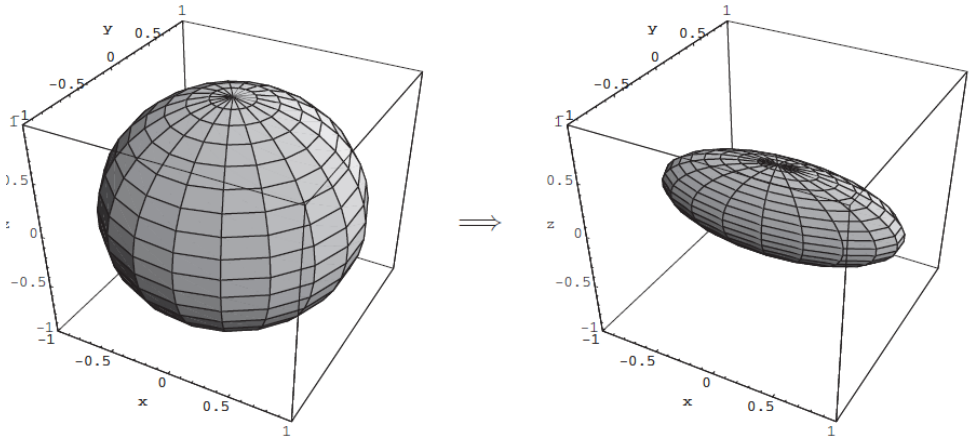

Figure 7.2: The effect of bit flip channel for p=0.3

It is important to note that the X operation is responsible for inducing the bit flip. As a result, the states along the x-axis remain unchanged, while the states along the y-axis and z-axis experience contraction by a factor of $1-2p$.

It is simpler to check specific details regarding quantum operations using this geometric image. It is simple to demonstrate that $\mathrm{tr}(\rho^2)$ is equal to $\frac{1+|r|^2}{2}$, where r is the bloch vector length. The contraction of the bloch sphere implies that the length of the bloch vector can only decrease so $\mathrm{tr}(\rho^2)$ can only ever decrease and the pure states get coverted to mixed states.

The phase flip channel has the following operation elements

$$E_0 = \sqrt{p}I = \sqrt{p}\begin{bmatrix}1 & 0\\ 0 & 1\end{bmatrix}, E_1 = \sqrt{1-p}Z = \sqrt{1-p}\begin{bmatrix}1 & 0\\ 0 & -1\end{bmatrix}$$

From a geometric perspective, the Bloch vector undergoes a projection along the z-axis, resulting in the loss of its x and y components.

The bit-phase flip channel, as its name suggests, combines both the bit flip and phase flip operations, given that $Y = iXZ$. The operation elements associated with this channel are presented below.

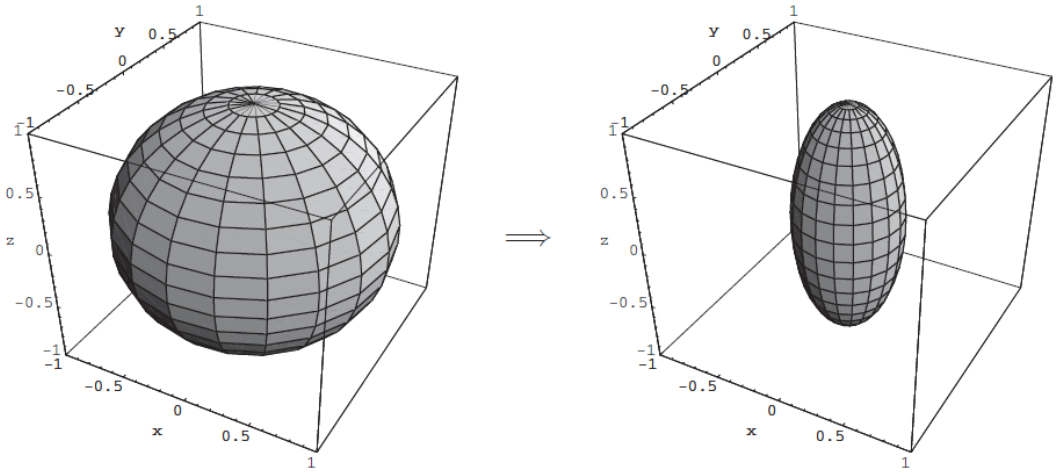

Figure 7.3: The effect of phase flip channel for p=0.3

$$E_0 = \sqrt{p}I = \sqrt{p}\begin{bmatrix} 1 & 0 \\ 0 & 1 \end{bmatrix}, E_1 = \sqrt{1-p}Y = \sqrt{1-p}\begin{bmatrix} 0 & i \\ -i & 0 \end{bmatrix}$$

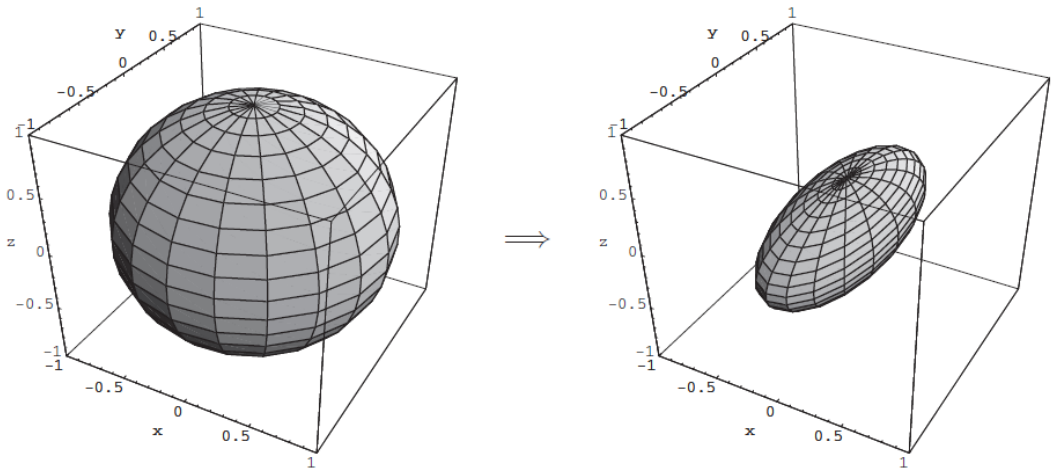

Figure 7.4: The effect of bit-phase flip channel for p=0.3

Notice that while the states along the x and z axes are reduced by a factor of 1-2p, the states along the y-axis are left unchanged.

7.2.3 Depolarizing channel

The depolarizing channel is a significant form of quantum noise that plays a crucial role in quantum information processing. Consider a single qubit, where there is a probability p that the qubit undergoes depolarization. In this case, the qubit is transformed into the completely mixed state,

represented by $I/2$, where I is the identity matrix. On the other hand, with a probability of $1-p$, the qubit remains unaffected. Consequently, the resulting state of the quantum system after the application of this noise can be described as a combination of the original state and the completely mixed state as given below:

$$\epsilon(p) = \frac{pI}{2} + (1-p)\rho \tag{7.2}$$

The effect of depolarizing channel on the bloch sphere is shown below. It is clear that the entire bloch sphere contracts as a function of p.

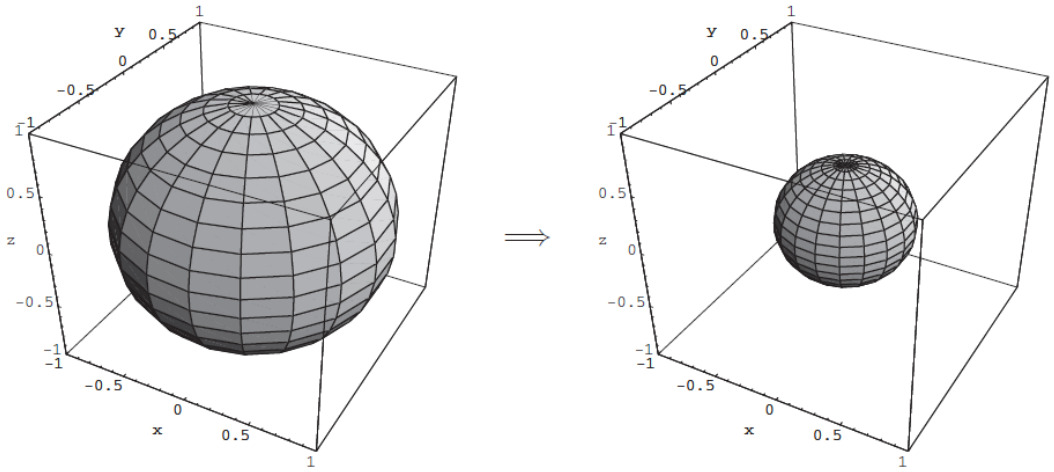

Figure 7.5: The effect of depolarizing channel for p=0.5

For an arbitrary ρ it is evident that we can write

$$\frac{I}{2} = \frac{\rho + X\rho X + Y\rho Y + Z\rho Z}{4} \tag{7.3}$$

$$\epsilon(p) = (1 - \frac{3p}{4})\rho + \frac{p}{4}(X\rho X + Y\rho Y + Z\rho Z) \tag{7.4}$$

which implies that the operation elements of the channel are $\sqrt{1-3/4}I$, $\sqrt{p}X/2$, $\sqrt{p}Y/2$, $\sqrt{p}Z/2$ which after conveniently parametrizing can be written as

$$\epsilon(p) = (1-p)\rho + \frac{p}{3}(X\rho X + Y\rho Y + Z\rho Z) \tag{7.5}$$

which has the interpretation that the density operator ρ is left alone with a probability $(1-p)$ and X,Y,Z operators are applied with probability $p/3$ which causes the entire bloch sphere to contract symmetrically.

The depolarizing channel can be expanded to encompass quantum systems with dimensions beyond two. The channel of depolarisation functions in a d-dimensional quantum system by replacing the quantum state with the fully mixed state I/d with a probability of p and keeping the state unchanged with a probability of 1-p. The quantum operation corresponding to this depolarizing channel can be described as follows: it transforms

the input state into a convex combination of the original state and the completely mixed state which is stated below:

$$\epsilon(p) = \frac{pI}{d} + (1-p)\rho \tag{7.6}$$

7.3 Applying noise model in Deuteron simulation

We can simply design our own noise model based on the characteristics of an actual quantum device using IBM's Qiskit Aer primitives. As we dont have the access to use the real hardware for many qubits so the most realistic result of the vqe simulation of deuteron is got by implementing a noise model to our otherwise nearly ideal simulation and then compare the results for fewer qubit hamiltonians in a real hardware. In this section first we would show the impact of a realistic noise model on the binding energy of deuteron for different qubit hamiltonian then implement two simple noise model designed by us on our simulation.

7.3.1 Impact of a realistic noise model on binding energy

In the chapter of deuteron we saw that using VQE for different qubits hamiltonian we got the binding energy value which was very close the experimental value. However it would not be the case if we run the same process on a real quantum hardware.There would be a significant deviation from the experimental result and sometimes the result may seem absurd. This happens because the simulation we are doing is like a closed quantum system where every process is unitary but when we are using real qubit hardware, the system qubits interacts with the environment and due to interaction the system is no longer closed and it becomes an open system and the dynamics is no longer governed fully by unitary. These interactions termed as noise can be modelled to be used in our simulation. Here we extract a realistic noise model data from the device(fake) backend which mimics real hardware. Shown below in the table are the binding energy results after adding noise.

No. of qubits in Hamiltonian	Expectation value of the Hamiltonian(Without Noise on simulator) in MeV	Expectation value of the Hamiltonian(With Noise on simulator) In MeV	Expectation value of the Hamiltonian (on real quantum hardware)In MeV
1	-0.43	-0.40	-0.34
2	-1.74	0.07	-0.53
3	-2.04	1.56	1.21
4	-2.14	5.42	Did not have access

Figure 7.6: Comparison of expectation value of hamiltonian with and without noise.

Given below are the plots of simulation comparing the effect of noise on the outcome of energy eigenvalue:-

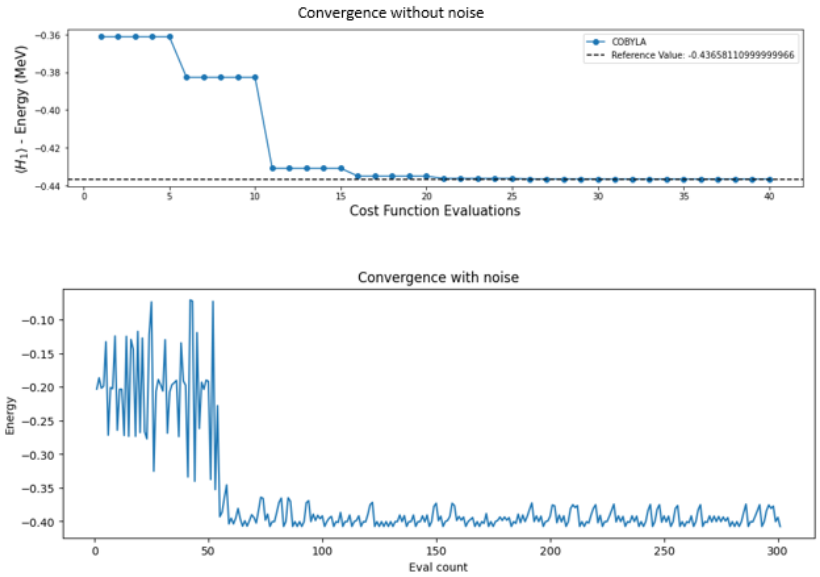

Figure 7.7: Comparing convergence of the expectation value of 1-qubit hamiltonian with and without noise.

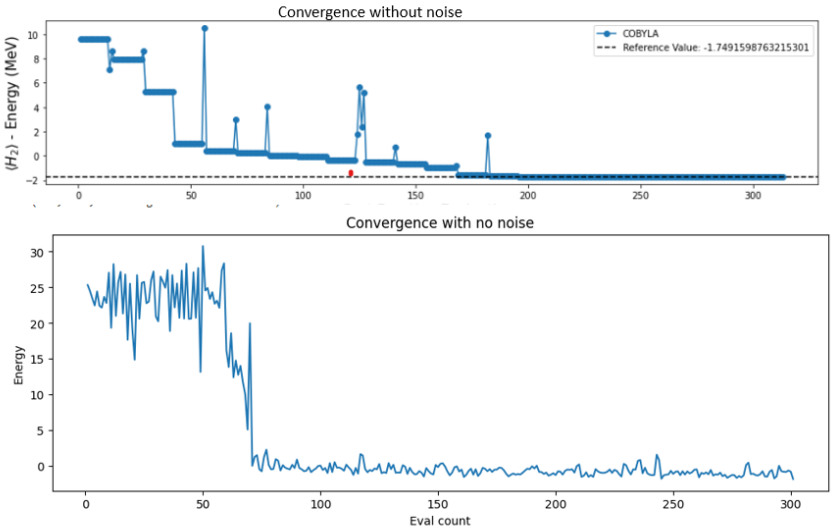

Figure 7.8: Comparing convergence of the expectation value of 2-qubit hamiltonian with and without noise.

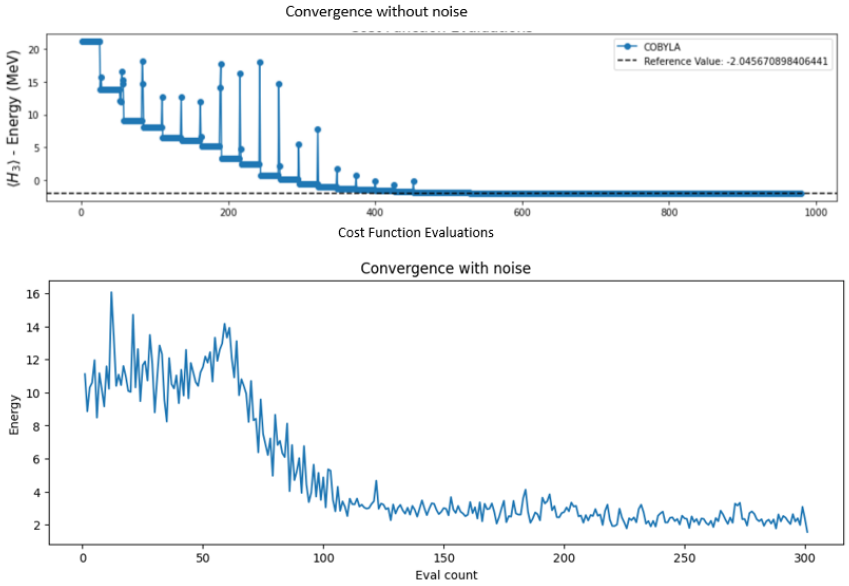

Figure 7.9: Comparing convergence of the expectation value of 3-qubit hamiltonian with and without noise.

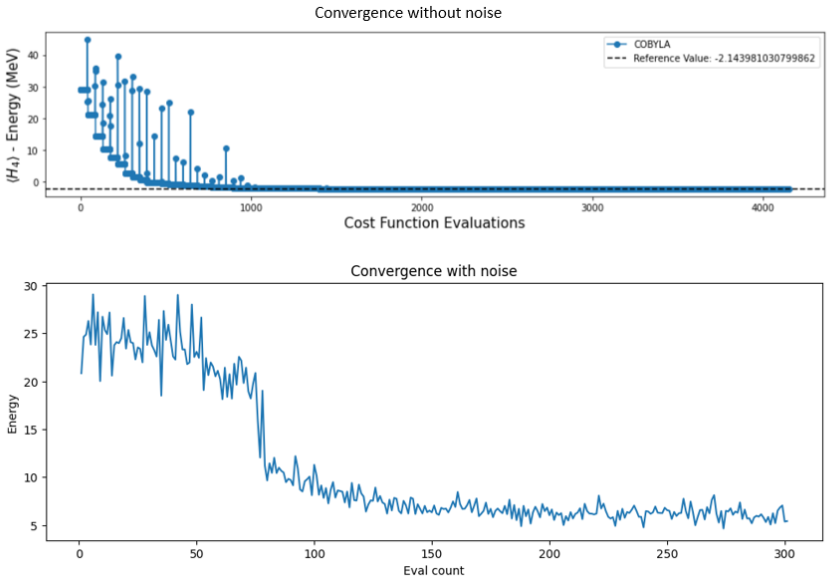

Figure 7.10: Comparing convergence of the expectation value of 4-qubit hamiltonian with and without noise.

7.4 Implementing our own simple noise model

After implementing the realistic noise model from device backend, we tried building my own noise model starting first with depolarising noise on all qubits and then using a all qubit bit flip noise channel to see how the result changes.

7.4.1 All qubit depolarising noise model

As discussed above the depolarising noise channel converts a pure state to a completely mixed state where X, Y ,Z gates applied with same probability. We build a depolarising channel where all the X,Y,Z gates act as an error with 5 percent on all qubits. Given below are the results of simulation after implementing this noise model.

No. of qubits in Hamiltonian	Expectation value of the Hamiltonian(Without Noise) in MeV	Expectation value of the Hamiltonian(With Depolarising Noise) In MeV
1	-0.43	-0.39
2	-1.74	2.01
3	-2.04	7.31
4	-2.14	12.28

Figure 7.11: Comparison of expectation value of hamiltonian with and without 5% depolarising noise on all qubits.

7.4.2 All qubit bit-flip noise model

Next we built a noise model where every bit is flipped from 0 to 1 and vice-versa with 5% probability. Basically the operator behind this noise model is X Pauli gate. Given below are the results of simulation after implementing this noise model.

No. of qubits in Hamiltonian	Expectation value of the Hamiltonian(Without Noise) in MeV	Expectation value of the Hamiltonian(With Bit-flip Noise) In MeV
1	-0.43	-0.41
2	-1.74	2.56
3	-2.04	8.22
4	-2.14	14.81

Figure 7.12: Comparison of expectation value of hamiltonian with and without 5% bit-flip noise on all qubits.

7.5 Remarks on the above results

It should be noticed here that without noise we are almost reaching the expected reference value. The accuracy increases with increasing qubit as more Pauli terms have contribution. With noise the results are significantly deviated and may seem absurd as sometimes the result of binding energy is coming out positive which conflicts the idea that deuteron is a bound system. However these would be nearly the results when we would be using a real quantum hardware as we did upto 3 qubits.With proper error mitigation schemes which is beyond the scope of this thesis. This results can be filtered to give meaningful outcomes.

8 A Model type approach

As extending the above method for a nucleus with more than two nucleon would be very complicated, the Potential energy term in the hamiltonian which is derived from Pionless Effective Field theory would involve three, four and even more body interaction terms. So we came across recent papers in Nature [10] and [11] where they thought of alpha as building block of some of the nucleus as Be-8, C-12. The obtained physical quantities exhibited good agreement with experimental data. This encouraged us to think if we could use Deuteron as the building block for Helium and do Quantum Simulation.

8.1 Deuteron clustering to form Helium

Helium has 2 protons and 2 neutrons. The angular momentum quantum no (l) is 0 from Shell Model calculations. So the Kinetic energy term would remain unchanged. Now for the potential energy we did grouping of nucleon into pairs to get the net interaction value.

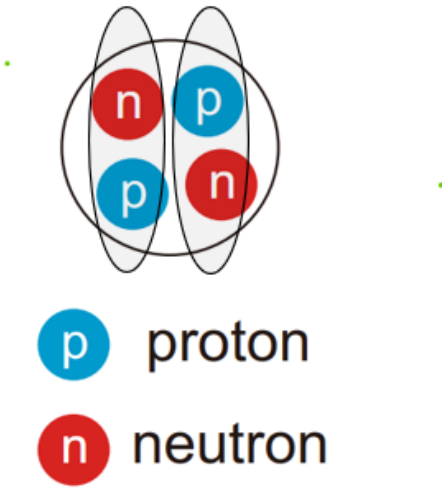

Figure 8.1: Deuteron clustering to form Helium.

Value of N	Value of Ground state energy(MeV)
1	-17.61
2	-20.68
3	-21.09
4	-21.25
5	-24.52
6	-26.69

Figure 8.2: Ground state energy values of helium for different qubit hamiltonian

So the value of V_0 changes to V_0' which is evident from the figure(8.1)given below. 6 different pairs can be formed taking two at a time. We repeated the above same calculation of Deuteron with an updated value of Potential energy matrix and hence updated hamiltonian which was mapped using JW transformation and created a variational circuit in Quantum computer upto N=6 to extract the results.

$$V_0' = 4C_2 * V_0 = 6 * (-5.68658111)MeV \tag{8.1}$$

Notice that although the results in Fig (8.2) are not very accurate, still the range of energy values are near experimental values which is $-28.3MeV$ which shows this the direction taken might be right!

9 Conclusion and Outlook

We have successfully explored the various aspects of the Variational Quantum Eigensolver algorithm , implementing it in the light nuclei like deuteron. The results are very satisfactory and indeed matches with the experimental values. This is not a novel work and previously there has been efforts along the same line. However, we extended this simulation to include certain types of Quantum noises. We studied the impact of these noise models on our simulated deuteron binding energy values. We even explored the impact of different ansatzes, encoding and entanglement pattern and studied their impact on the convergence of my results. Inspite of limiting ourself to only the ground state, we explored an algorithm called Subspace Search Variational Quantum Eigensolver for excited states and implemented it on our deuteron problem to infer that deuteron becomes unbounded system when it is not in the ground state. Towards the end we tried applying VQE to heavier nuclei with a model type approach of deuteron clustering. Although the results of the heavier nuclei are not exact like deuteron, the range looks very optimistic. Recent efforts have been made on a diagonalisation process, theory and calculations of which are discussed in the Appendix would be part of future works of implementing Quantum computers in high energy physics. It should also be noted that at this time we are in the NISQ era and are bound by the no of quantum processors. However there are continuous efforts in increasing the powers of Quantum processors by increasing the number of stable qubits. So the days are not far away when Quantum computers can do non trivial tasks which becomes intractable for classical computers and all these works would help the mankind to explore new things.

A

Schrieffer Wolff Transformation on Quantum devices

Controlling quantum many-body system is highly importance in various fields of physics. In most of the application low energy effective Hamiltonian(H_{eff}) is enough in describing the required physics for applications. Schrieffer-Wolff transformation is such a perturbative approach which is used in condensed matter, quantum optics and quantum electrodynamics to calculate the low energy effective Hamiltonian by comprehending the renormalization effects of strong correlations in the quantum many-body models. However, the most crucial part in SWT is the calculation of the generator which is generally done by heurestic method. Here inspired by the recent papers [12]and [13], we would show the mathematical steps and discuss the algorithm using which the generator can be easily calculated and would be explicitly be shown for Single Impurity Anderson model and Jayes Cummings model. The authors of the above papers are the first to carry out a fully quantum algorithm of this kind. Taking inspiration from the above work, we do all the necessary mathematical steps and would try to implement the above ideas in solving some high energy physics hamiltonians or in exploring nuclear structures in the near future.

A.1 Mathematical steps:-

$$U = e^{\varepsilon S} = \sum_{k=0}^{\infty} \frac{(\varepsilon S)^K}{k!} \approx 1 + \varepsilon S + \frac{\varepsilon^2 S^2}{2}$$

Similarly,

$$U = e^{-\varepsilon S} = \sum_{k=0}^{\infty} \frac{(-\varepsilon S)^K}{k!} \approx 1 - \varepsilon S + \frac{\varepsilon^2 S^2}{2}$$

Here we ensure $S^\dagger = -S$ so that $U^\dagger U = I$

Transforming the hamiltonian, we can write

$$H \approx (1 + \varepsilon S + \frac{\varepsilon^2 S^2}{2}) H (1 - \varepsilon S + \frac{\varepsilon^2 S^2}{2}) \tag{A.1}$$

$$\approx H + \varepsilon(SH - HS) + \frac{\varepsilon^2}{2}(S^2 H + HS^2 - 2SHS) \tag{A.2}$$

$$\approx H + \varepsilon[S, H] + \frac{\varepsilon^2}{2}[S, [S, H]] \tag{A.3}$$

The above equation is the special result of BCH formula which allows us to handle exponential of operators in quantum mechanics as due to the non-commuting nature of operators, we cant simply use exponent laws. Let us define a hamiltonian which involves a diagonal term H_0 and an off diagonal perturbative term H_1 and the small perturbation parameter be ε. Next we transform the hamiltonian to a different frame H' which makes the problem easier to solve and might give better insights of the Quantum mechanical system.

$$H = H_0 + \varepsilon H_1 \tag{A.4}$$
$$H' = e^{\varepsilon S} H e^{-\varepsilon S}$$

$$\begin{aligned} H &\approx H + \varepsilon[S, H] + \frac{\varepsilon^2}{2}[S, [S, H]] \\ &\approx H_0 + \varepsilon H_1 + \varepsilon[S, H_0 + \varepsilon H_1] + \frac{\varepsilon^2}{2}[S, [S, H_0 + \varepsilon H_1]] \\ &\approx H_0 + \varepsilon(H_1 + [S, H_0]) + \frac{\varepsilon^2}{2}[2[S, H_1], [S, [S, H_0]]] \end{aligned}$$

By choosing S(anti hermitian) we can make the second term 0 which means $H_1 = -[S, H_0]$ transforms the hamiltonian into the frame of our convenience. We can also choose $\varepsilon = 1$ then the final form of the hamiltonian is

$$H' = H_0 + \frac{[S, H_1]}{2} \tag{A.5}$$

We see that the above equation is not exactly equal to H but does give some insights of the complex Quantum mechanical system by absorbing the information of the off-diagonal part into the original diagonal chunk to give a new diagonal matrix. Thus SWT is an operator version of the second order perturbation theory whose approximation helps us go very far in describing the system's time evolution.

A.2 Quantum Algorithm for SWT

In reference with the paper[12], a fully quantum algorithm is made which helps in calculating the generator using quantum devices. The steps are as follows: 1)First we have take the hamiltonian in the second quantised form of the many body problem which we are interested in.

2)To convert the above hamiltonian to quantum operators form (H_q) which can be well understood by quantum computers, we do Jordan Wigner mapping.
3)The qubit hamiltonian form can be written into two parts which are the diagonal(H_q^d)and off-diagonal (H_q^{od}).

$$H_q = H_q^d + H_q^{od}$$

4)Next the commutation relation $\eta_q = [H_q^d, H_q^{od}]$ should be calculated which gives the qubit form of the generator S_q but the coefficients remain unknown.
5)To know the coefficient the second term of the BCH formula which we equated to 0 should be calculated $H_q^{od} = -[S, H_q^d]$.
6)After we have the final form of the generator in the qubit form we incorporate that in the eqn(9.5) to get the effective hamiltonian in the qubit operator form.

$$H_{eff} = H_q^d + \frac{[S, H_q^{od}]}{2} \tag{A.6}$$

.

A.3 Implementation of SWT and its quantum algorithm

The SWT was implemented in the Single Impurity Anderson Model(SIAM) and Jayes Cummings model to find the generator. Also the quantum algorithm of the SWT for implemented in the SIAM model using Qiskit. Given below are few steps of the calculations and results:-

A.3.1 Analytical calculation on Single Impurity Anderson model's hamiltonian

The hamiltonian of the SIAM model consisting of electron in conduction band and impurities is given below:-

$$H = \sum_{k,\sigma} \epsilon_k c_{k\sigma}^\dagger c_{k\sigma} + \sum_{\sigma} \epsilon_d d_\sigma^\dagger d_\sigma + \sum_{k,\sigma} V_k (c_{k\sigma}^\dagger d_\sigma + d_\sigma^\dagger c_{k\sigma}) + U n_{d\uparrow} n_{d\downarrow} \tag{A.7}$$

The first term in the hamiltonian corresponds to electron in the conduction band. The second term corresponds to the impurity while the third term is called the coupling part of the hamiltonian showing the coupling between electron and the impurity. The last term corresponds to coulombic repulsion. The above hamiltonian can be broken into a diagonal and off-diagonal part which are

$$H^d = \sum_{k,\sigma} \epsilon_k c_{k\sigma}^\dagger c_{k\sigma} + \sum_{\sigma} \epsilon_d d_\sigma^\dagger d_\sigma + U n_{d\uparrow} n_{d\downarrow}$$

$$H^{od} = \sum_{k,\sigma} V_k(c^\dagger_{k\sigma} d_\sigma + d^\dagger_\sigma c_{k\sigma})$$

Next following the step of the algorithm we calculate the value of

$$\begin{aligned}\eta &= [H^d, H^{od}] \\ &= \sum_{k,\sigma} (\epsilon_k - \epsilon_d - U n_{d\bar{\sigma}}) V_k (c^\dagger_{k\sigma} d_\sigma - d^\dagger_\sigma c_{k\sigma})\end{aligned}$$

So the generator of the SWT should be

$$s == \sum_{k,\sigma} (A_k - B_k n_{d\bar{\sigma}}) V_k (c^\dagger_{k\sigma} d_\sigma - d^\dagger_\sigma c_{k\sigma}) \tag{A.8}$$

where the unknown coefficients would be determined by imposing the condition which removes the off diagonal term to the first order of BCH formula

$$[S, H^o] = -H^{od} \tag{A.9}$$

Calculating the above equation and comparing it with the off diagonal part of hamiltonian we get the following value of the unknown coefficients.

$$A_k = \frac{1}{\epsilon_k - \epsilon_d} \tag{A.10}$$

$$B_k = \frac{1}{\epsilon_k - \epsilon_d - U} - \frac{1}{\epsilon_k - \epsilon_d} \tag{A.11}$$

Now these unknown coefficients can be put in the generator to calculate the effective hamiltonian H_{eff}.

A.3.2 Analytical calculation on Jaynes Cummings hamiltonian in rotating wave approximation

The hamiltonian is given as:-

$$\frac{H}{\hbar} = \omega_r a^\dagger a - \frac{1}{2}\omega_q Z + g(a^\dagger \sigma^- + a\sigma^+)$$

(A.12)

Here the first term in the hamiltonian corresponds to number of photons in the resonator, the second term corresponds to the state of the qubit and the final term is the coupling term. a and $a^\dagger$ are the photon annihilation and creation operator, $\sigma^+$and σ^-)are the qubit raising and lowering operator such that $\sigma^+ = \frac{X+iY}{2}$ and $\sigma^- = \frac{X-iY}{2}$. The diagonal and off-diagonal term of the hamiltonian are:-

$$H^d = \omega_r a^\dagger a - \frac{1}{2}\omega_q Z$$

$$H^{od} = g(a^\dagger \sigma^- + a\sigma^+)$$

Using proper commutation relations between Pauli operators, we calculate the value of

$$\eta = [H^d, H^{od}] \tag{A.13}$$
$$= g(\omega_r + \omega_q)a^\dagger \sigma^- - g(\omega_r + \omega_q)a\sigma^+ \tag{A.14}$$

So the generator of the SWT should be

$$S = Aa^\dagger \sigma^- + B(\omega_r + \omega_q)a\sigma^+ \tag{A.15}$$

The value of the unknown constants can be found by using the same eqn(9.9),

$$A = \frac{g}{\omega_r + \omega_q}, B = \frac{-g}{\omega_r + \omega_q}$$

So the generator S is obtained and now substituting S in eqn(9.6) the value of H_{eff} can be found.

A.3.3 Implementing the quantum algorithm

Next we show the calculation of the quantum algorithm of SWT on 2-site SIAM hamiltonian which is given below:-

$$H = Un_{1\uparrow}n_{1\downarrow} - \epsilon_1 \sum_\sigma n_{1\sigma} + \sum_\sigma c^\dagger_{2\sigma}c_{2\sigma} + \sum_\sigma V(c^\dagger_{1\sigma}c_{2\sigma} + c^\dagger_{2\sigma}c_{1\sigma}) \tag{A.16}$$

$$H_q = U(a_1^\dagger a_1 \times a_3^\dagger a_3) + V(c_1^\dagger c_2 + c_2^\dagger c_1 + c_3^\dagger c_4 + c_4^\dagger c_3) - \epsilon_1(a_1^\dagger a_1 + a_3^\dagger a_3) + \epsilon_2(c_2^\dagger c_2 + c_4^\dagger c_4) \tag{A.17}$$

Next we map the hamiltonian into the pauli operators (X,Y,Z) form using Jordan Wigner transformation so that it can be understood by the quantum computer.

$$H_q = \frac{U}{4}(Z_1Z_3) + (\frac{\epsilon_1}{2} - \frac{U}{4})(Z_1 + Z_3) - \epsilon_2(Z_2 + Z_4) + \frac{V}{2}(X_1X_2 + Y_1Y_2 + X_3X_4 + Y_3Y_4) \tag{A.18}$$

The diagonal and off diagonal part of the hamiltonian are:-

$$H_q^d = \frac{U}{4}(Z_1Z_3) + (\frac{\epsilon_1}{2} - \frac{U}{4})(Z_1 + Z_3) - \epsilon_2(Z_2 + Z_4)$$

$$H_q^{od} = \frac{V}{2}(X_1X_2 + Y_1Y_2 + X_3X_4 + Y_3Y_4)$$

Next we calculate the commutation relation and use the appropriate pauli operators commutation relations below

$$\eta_q = [H_q^d, H_q^{od}]$$

$$\eta_q = \frac{iUV}{4}(Z_3(Y_1X_2-X_1Y_2)+Z_1(Y_3X_4-X_3Y_4))+(iV(\frac{\epsilon_1}{2}-\frac{U}{4})+\frac{i\epsilon_2 V}{2})(Y_1X_2-X_1Y_2+Y_3X_4-X_3Y_4) \tag{A.19}$$

Thus the generator of SWT should be of the form:-

$$S_q = A(Y_1X_2 - X_1Y_2)(1 - Z_3) + B(Y_3X_4 - X_3Y_4)(1 - Z_1) \tag{A.20}$$

The above coefficients acn be determined using the relation

$$H_q^{od} = -[S, H_q^d]$$

Thus the unknown coefficients are:-

$$A = \frac{-iV}{4U(1 - Z_3)}$$

$$B = \frac{-iV}{4U(1 - Z_1)}$$

Once we got the generator we can now easily get the effective hamiltonian in the qubit form which can be given as an input to quantum computers to study the underlying physics.

A.4 Remarks on the above results

The above results show that using the fully quantum algorithm we can find the generator of SWT easily which in turn helps us in diagonalising the difficult hamiltonian keeping the underlying physics intact. So yet again quantum computer finds an interesting application in physics. Our goal would be to use this algorithm developed by the authors of the above papers in a complex high energy physics hamiltonian in the near future.

References

[1] R. P. Feynman, "Simulating physics with computers," in *Feynman and computation*, CRC Press, 2018, pp. 133–153.

[2] S. Popescu, "Bell's inequalities versus teleportation: What is nonlocality?" *Physical review letters*, vol. 72, no. 6, p. 797, 1994.

[3] M. A. Nielsen *et al.*, "The fermionic canonical commutation relations and the jordan-wigner transform," *School of Physical Sciences The University of Queensland*, vol. 59, 2005.

[4] T. Papenbrock, "Quantum computing of atomic nuclei," *Bulletin of the American Physical Society*, vol. 63, 2018.

[5] S. A. Coon and M. K. Kruse, "Properties of infrared extrapolations in a harmonic oscillator basis," *International Journal of Modern Physics E*, vol. 25, no. 05, p. 1 641 011, 2016.

[6] S. König, S. Bogner, R. Furnstahl, S. More, and T. Papenbrock, "Ultraviolet extrapolations in finite oscillator bases," *Physical Review C*, vol. 90, no. 6, p. 064 007, 2014.

[7] K. M. Nakanishi, K. Mitarai, and K. Fujii, "Subspace-search variational quantum eigensolver for excited states," *Physical Review Research*, vol. 1, no. 3, p. 033 062, 2019.

[8] A. Rivas and S. F. Huelga, *Open quantum systems*. Springer, 2012, vol. 10.

[9] M. A. Nielsen and I. Chuang, *Quantum computation and quantum information*, 2002.

[10] T. Otsuka, T. Abe, T. Yoshida, *et al.*, "α-clustering in atomic nuclei from first principles with statistical learning and the hoyle state character," *Nature Communications*, vol. 13, no. 1, p. 2234, 2022.

[11] D. Jenkins, "Alpha clustering in nuclei: Another form of shape coexistence?" *Journal of Physics G: Nuclear and Particle Physics*, vol. 43, no. 2, p. 024 003, 2016.

[12] R. U. Haq, B. Iqbal, M. Illahi, B. Ahmad, *et al.*, "Schrieffer-wolff transformation on ibm quantum computer," *arXiv preprint arXiv:2208.04746*, 2022.

[13] R. U. Haq and K. Singh, "A systematic method for schrieffer-wolff transformation and its generalizations," *arXiv preprint arXiv:2004.06534*, 2020.

[14] J. Tilly, H. Chen, S. Cao, *et al.*, "The variational quantum eigensolver: A review of methods and best practices," *Physics Reports*, vol. 986, pp. 1–128, 2022.

[15] S. More, A. Ekström, R. Furnstahl, G. Hagen, and T. Papenbrock, "Universal properties of infrared oscillator basis extrapolations," *Physical Review C*, vol. 87, no. 4, p. 044 326, 2013.